An assessment of site response from the study of the *H*/*V* ratios in the Garhwal Himalaya, India

K. Sivaram* and S. S. Rai

National Geophysical Research Institute (CSIR), Uppal Road, Hyderabad 500 007, India

The Garhwal Himalaya region with moderate to high seismicity has considerable seismic risk potential arising from complex tectonic evolutionary processes. We assess first approximations of site responses across the region using the empirical horizontal to vertical (*H*/*V*) spectral amplitude ratio method of Nakamura (1989). The data comprises recorded ambient seismic noise and local earthquakes using a network of digital broadband seismographs from June 2005 to June 2008. The site response is calculated as the *H*/*V* amplitude spectra at each site following the hypothesis of Nakamura. These spectra are used in estimating site-specific fundamental resonance frequencies and peak amplitudes. The stability of the *H*/*V* ratio is studied using standard deviations and 90% confidence intervals. Our results show that seasonal variations in the ambient noise data do not affect frequency estimates. The 'peak' corresponding to fundamental resonance frequency, is prominently present in both ambient noise and earthquake datasets. Observed *H*/*V* ratios correspond to the effects of velocity contrast and characteristic sub-surface topographic effect around a certain frequency range. Estimated fundamental resonance frequencies are in the range 2–5 Hz for the studied sites. Our results provide valuable inputs for further studies on site characterization and damage mitigation.

Keywords: Ambient noise, Garhwal Himalaya, *H*/*V* spectral ratio, site response.

LOCAL site conditions, such as upper soil surface cover may cause abrupt changes in recorded intensities of earthquakes and damages in the affected area. Physical parameters such as impedance changes from velocity gradient, energy trapping from 'soft' layer, and surface topography effects cause variations in seismic wave propagation. Site response studies, as first part of seismic hazard and microzonation studies, are aimed at understanding seismological response from the upper layers of soil and thereby, interaction with local structures. Our site response study pertains to locations along the cross-section of the Garhwal Himalaya, which has been the site of moderate earthquakes, prominent being the one on March 1999 with *M* 6.3, epicentral location 30.40°N, 79.416°E, in the Chamoli region. Recorded intensities of this earthquake have shown large spatial variability due to varying site conditions[1]. Also, the region is continuously experiencing small to moderate magnitude earthquakes, increasing the potential of seismic risk, as observed from several studies[2,3] close to the surface trace of the Main Central Thrust (MCT), especially near some of the study locations. Most of the seismological studies conducted in the Himalaya region are aimed at studying seismo-tectonics and crustal scale imaging[4–6]. It is therefore necessary to provide fresh information of site response needed for seismic hazard analysis. A non-invasive, empirical site response technique, using ambient noise which has turned out to be a useful structural engineering tool is the *H*/*V* spectral ratio, as re-modified by Nakamura[7]. The most attractive feature of this technique is the low-cost applicability to a single station, even in regions of moderate to low seismicity. Further studies such as Lermo and Garcia[8] showed the applicability of Nakamura's method in site response studies. In general, such site response studies are used to determine fundamental frequency of seismic ground motion at unconsolidated sites. A few studies in the Garhwal region, such as Nath *et al.*[9] have used aftershock data and five seismographs placed within 20 km radius of the Chamoli earthquake source region. *H*/*V* spectral ratio based on ambient seismic noise, is useful in studying possibility of sub-surface velocity structure without need for infrequent earthquakes or expensive explosions.

Garhwal Himalaya is the result of a long geological evolution, with a vast stretch of geodynamic complexity and plate-collisionary deformation, where the Indian plate is underthrusting beneath the Eurasian plate[3]. From the vast literature available on the Himalayan geodynamics, one can infer a continual trend of accumulation of

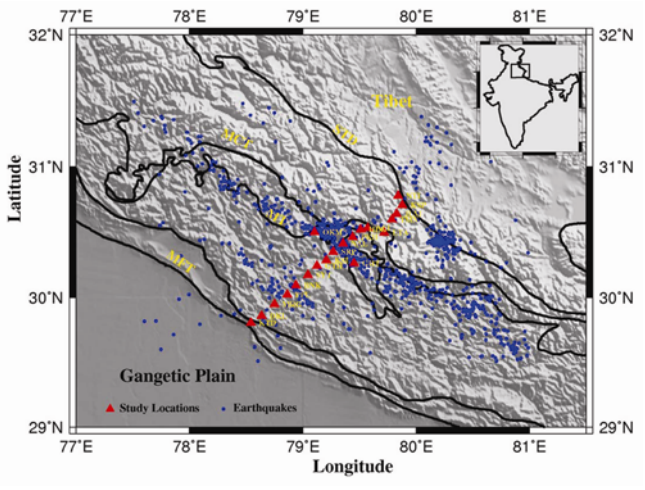

Figure 1. Physiographic map of the study region in the Garhwal Himalaya, India. Red triangles show the locations of investigated sites. Blue circles show the seismicity observed in region from 1990 to 2008 (source: USGS and earthquakes recorded over our broadband seismograph network from 2005–2008). STD, Southern Tibetan Detachment; MCT, Main Central Thrust; MT, Munsyari Thrust; MBT, Main Boundary Thrust; MFT, Main Frontal Thrust.

*For correspondence. (e-mail: sivaramk@ngri.res.in)

strain energy in the complex geodynamic zone. The region is seismically active, even though there have not been high magnitude earthquakes. Figure 1 shows dense seismicity patterns (shown by blue circles) in a tectonic map of the study region, from our earthquake data recorded over our broadband stations, and also US Geological Survey (USGS) earthquake data during 1990–2008. Several major thrust planes such as the Southern Tibetan Detachment (STD), MCT, the Munsyari Thrust (MT), the Main Boundary Thrust (MBT) and the Main Frontal Thrust (MFT) are expressions of geodynamic complexity.

The Lesser Himalaya is structurally bounded by MBT and MCT. It consists mainly of Precambrian clastic sediments. The greater Himalaya is bounded by MCT and STD and comprises early Cambrian metasedimentary rocks. In geological perspective of the sedimentary deposits, MCT places high-grade gneisses (Greater Himalaya) on top of lower-grade schists (Lesser Himalaya), whereas MBT juxtaposes those schists against the unmetamorphosed Miocene–Plestocene molasses (the Siwalik Group). The detailed geological perspective is presented in the literature[10–12].

Nakamura[7] defined site response, using long-duration three-component ambient noise records (or weak seismic motion), as a quasi-transfer function involving the ratio of the combined horizontal amplitude spectrum (H) to vertical amplitude spectrum (V) at the studied site. The horizontal-to-vertical spectral ratio (HVSR) method is an empirical single-station site-response approach to basically estimate fundamental frequency of a site.

For sub-surface site conditions showing a velocity contrast, the H/V amplitude versus frequency curve shows a peak, which if sufficiently clear, closely corresponds to fundamental frequency of the unconsolidated site. On the other hand, maximum amplitude of the peak may not directly relate to the actual site amplification, but depends upon the characteristics of the unconsolidated layer and its layout with respect to the bedrock. The hypothesis assumes vertically propagating and horizontally polarized shear wave propagation in the 'soft' layer near surface, as in many basin structures. Also, according to the hypothesis, the vertical component is not amplified, and the source and path effects are removed. Under such conditions, Nakamura technique provides a reliable estimate of the site resonance frequency, as compared to other methods which require a reference site. Besides, it provides information related to sub-surface soil properties through the well-known formula $f_0 = V_s/4H$, where f_0 = fundamental resonance frequency, V_s is the shear velocity near the surface and H is the depth up to the basement. Several studies[13,14] have shown the correlation between the peak on H/V curve and impedance contrast of the underlying media. Bard and SESAME Team[15] performed detailed studies and concluded that the H/V peak (or peaks) arises from a multitude of causes such as Rayleigh wave ellipticity, airy phase of Love wave modes and resonance of body waves, whereas the original Nakamura-hypothesis is based on multiple reflections of the SH waves. However, the recent studies by Bonnefoy-Claudet *et al.*[16] showed that independent of the body-wave or surface-wave model, H/V spectral ratio curves generally exhibit a peak in the vicinity of the fundamental resonance of the soil, and that the relative proportion of different seismic waves is controlled by the impedance contrast in underlying media. Frequency-dependent site amplification has also been repeatedly observed on top of rocky hills, valley edges and sloping surfaces[17–20].

Our data source is derived from broadband seismographs at 20 locations (Figure 1) from June 2005 to June 2008, covering regions from Lower Himalaya to Higher Himalaya, along a linear profile from KTD (Kotdwar) to NTI (Niti). We used Guralp CMG-3T broadband seismometer (120 s, 50 Hz) and Reftek RT-130/1 digital recording system (24-bit output resolution) for continuous recording of time series data at 50 samples/s for over 20 months, which were synchronized by means of a Global Positioning System (GPS) reference time. We eliminated instrument effect and used 'GEOPSY' software (GEOPhysical Signal database for noise arraY processing) (http://www.geopsy.org), developed under the SESAME (Site EffectS assessment using AMbient Excitations) project (SESAME European Research Project, 2005). We studied variability of H/V ratios during different seasons and record lengths, in frequency range of 0.5–15 Hz. We used two variations of ambient noise data: One hour was the minimum record length and 48 h were the maximum record length considered. We selected a large number (>30) of time windows (each of 60 s) and applied on each component spectrum, a cosine function tapering of width 0.05 to avoid spectral leakage, Konno and Ohmachi logarithmic filter with a moderate smoothing constant at 40. The horizontal amplitude spectra, H are calculated as the quadratic mean of Fast Fourier Transform (FFT) spectra of the N–S and E–W components. The vertical amplitude spectra (V) are similarly calculated from the vertical component for each time window. The final H/V ratio is obtained after averaging the values of H/V ratios of all the time windows.

To study the effect of temporal variations, a total of 30 different noise data samples covering the entire study period (June 2005–June 2008) at each site were thus compiled. To account for variability in the H/V ratios, we computed the estimated parameters from all the observed H/V ratios having different characteristic H/V curves. The frequency and amplitude estimate of the peak, at which the maximum H/V occurs, were studied for stability using standard deviations and 90% confidence intervals (CI). As the H/V method depends upon velocity contrast for its unambiguous peak, the presence of lateral heterogeneities and surface topography might hinder its quality factor in terms of the peaks, their 'width' (or frequency band) and 'height' (or amplitudes). Numerical studies on two-

Table 1. Details of the studied sites in Kumaon Himalaya

Site Name	Latitude (°N)	Longitude (°E)	Altitude (m)	Near-surface details at recording station
ALI (Auli)	30.531	79.572	2658	Hill top (flat topography); Stiff soil
BNK (Banekh)	30.091	78.938	1405	Hill top (flat topography); Rock
DKL (Devikhal)	29.855	78.636	1236	Gentle hill slope; Rock
GTH (Geithi)	30.243	79.123	1579	Hill top (flat topography); Rock.
GHT (Ghat)	30.263	79.452	1489	Hill top (edge of valley); Stiff soil
HLG (Hilang)	30.519	79.509	1627	Hill top (edge of valley); Rock
JLM (Jelum)	30.639	79.825	2915	Hill slope (edge of valley); Soft soil
KSL (Khaskhal)	30.285	79.207	1451	Hill slope (edge of valley); Rock
KSP (Kailashpur)	30.707	79.877	3115	Hill slope (flat area); Stiff soil
KTD (Kotdwar)	29.804	78.542	1074	Hill top (flat topography); Rock
LTA (Lata)	30.495	79.717	2362	Mountain slope; Rock
MRG (Murgaon)	29.948	78.748	805	Hill top (flat topography); Rock.
NAL (Nail)	30.412	79.353	1303	Hill top (flat topography); Rock
NTI (Niti)	30.778	79.840	3065	Gentle hill slope; Rock
OKM (Okhimath)	30.500	79.103	1525	Hill slope (flat area); Rock
PKH (Pakhi)	30.461	79.440	1584	Hill slope; Rock
PPL (Pipli)	30.021	78.862	1292	Hill top (flat topography); Rock
SRP (Siropani)	30.349	79.267	1490	Hill top (flat area); Rock
SYT (Syolitalli)	30.172	79.045	1681	Hill top (flat area); Stiff soil
TMN (Tamaknala)	30.595	79.784	2541	Hill slope (edge of valley); Rock

Table 2. Estimated parameters of site responses as evaluated by the ambient noise *H*/*V* ratio method

	H/*V* Site response (ambient noise) (June 2005–June 2008)	
Site name	$f_{H/V} \pm 1\sigma$, Hz	Max. (mean) *H*/*V* ± 90% CI
ALI (Auli)	0.897 ± 0.672	2.801 ± 2.860
BNK (Banekh)	Flat peak	< 2
DKL (Devikhal)	5.040 ± 0.330	2.266 ± 0.117
GTH (Geithi)	7.823 ± 0.827	< 2
GHT (Ghat)	5.333 ± 0.353	3.835 ± 0.145
HLG (Hilang)	2.045 ± 0.035	2.572 ± 0.077
JLM (Jelum)	1.845 ± 0.025	3.746 ± 0.095
KSL (Khaskhal)	Flat peak	< 2
KSP (Kailashpur)	2.692 ± 0.045	3.783 ± 0.088
KTD (Kotdwar)	1.232 ± 0.063	2.721 ± 0.078
LTA (Lata)	Flat peak	< 2
MRG (Murgaon)	4.011 ± 0.042	< 2
NAL (Nail)	2.045 ± 0.120	4.040 ± 0.059
NTI (Niti)	2.843 ± 0.081	< 2
OKM (Okhimath)	9.874 ± 0.668	2.293 ± 0.026
PKH (Pakhi)	Flat peak	< 2
PPL (Pipli)	7.545 ± 0.158	2.573 ± 0.079
SRP (Siropani)	Flat peak	< 2
SYT (Syolitalli)	3.928 ± 0.059	3.402 ± 0.059
TMN (Tamaknala)	2.990 ± 0.073	4.687 ± 0.189

dimensional and three-dimensional structural models[17,19,20] predict that other than the horizontally flat locations (which are commonly encountered in urban areas), significant site effects are also possible on the flat parts of hill tops or hilly edges with strong lateral variation and the corresponding *H*/*V* curves exhibit low to significant maxima. 'Ideal rock' sites, with flat topography, which have a low and flat response are found to have a peak *H*/*V* ratio around 1.

The surface features at the 20 study locations are described in Table 1. The corresponding estimated site responses using ambient noise are detailed in Table 2. It also shows the variability in *H*/*V* amplitudes that was studied by means of standard deviations and 90% CI. The sites situated above the MCT region, which have shown responses with clear, stable and strong 'peaks' are: ALI, HLG, KSP, JLM and TMN (details in Table 1). In Figure 2, we see that all sites have clear response at well-defined fundamental frequencies, whereas site NTI has shown low amplitude response. The lower frequency estimate at which the clear peak is stable is defined as fundamental frequency, whereas the fuzzy (ambiguous) or multiplicity of peak trend is attributed to lateral variations. Similarly, sites located below MCT, which have shown frequency-dependent sensitivity are DKL, MRG, PPL, SYT, GHT, KTD, NAL (Figure 3).

Observed *H*/*V* ratios are shown in grey lines, whereas the corresponding averaged (mean) *H*/*V* ratios are shown in red lines. Variations in the estimated peak *H*/*V* amplitudes are shown with 90% CI limits in blue dashed lines, whereas $\pm 1\sigma$ (standard deviations) are shown in thick black lines. Fundamental peaks are seen remarkably stable with low standard deviations and good clarity criteria. These well-defined frequency-dependent peaks correspond to layers of sediment deposits overlying hardrock basements. Some site responses have also shown slightly 'broad' or multiplicity of peaks such as the site GHT (Figure 3 *a*).

The topographical setting explains the occurrence of broad and multiple peak *H*/*V* curves, and is the relatively predominant effect of a deep underground sloping as the stations are found on hill and valley edges. The prominent peak at 5.333 Hz for GHT, or lower cutoff frequency

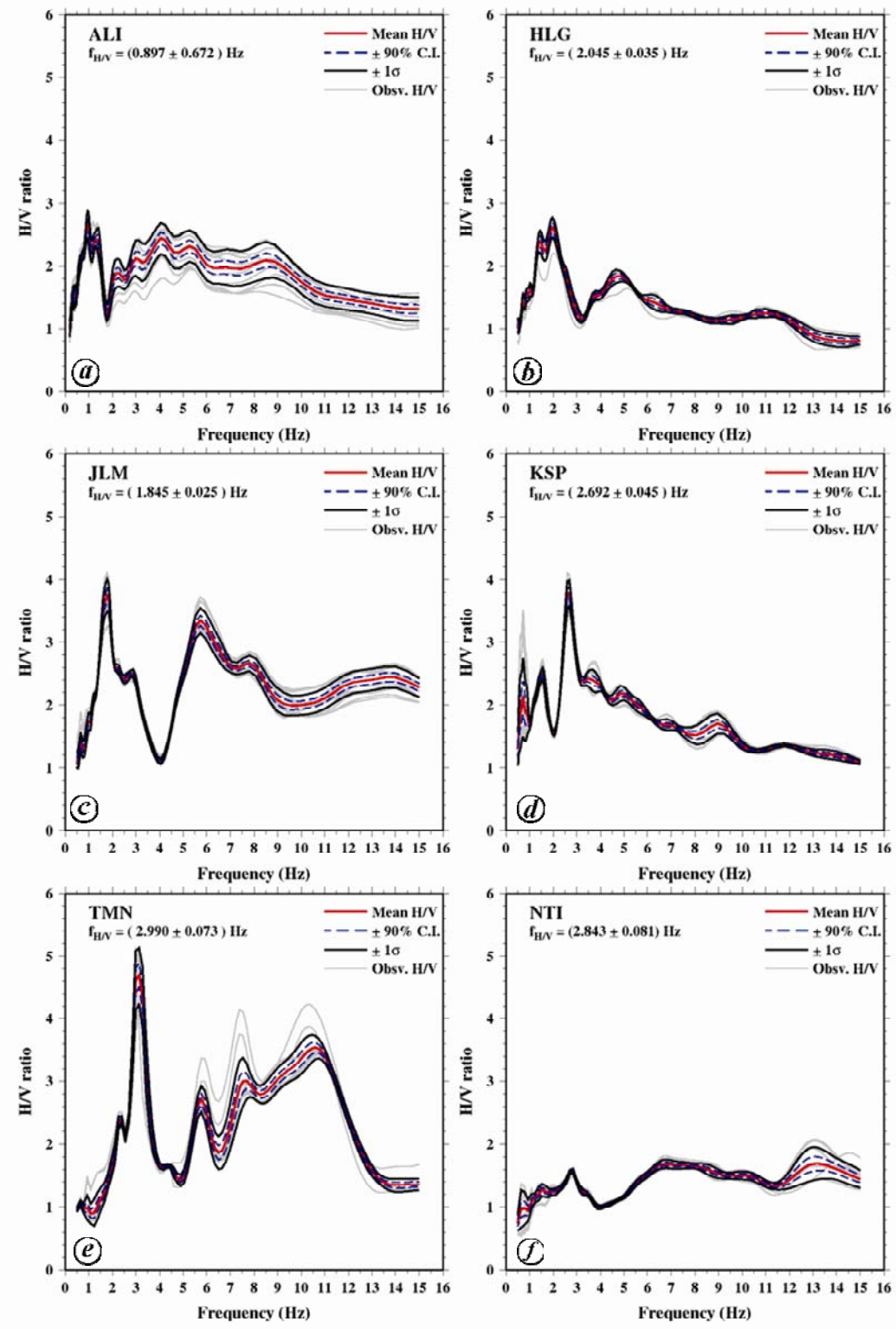

Figure 2. Sites located above MCT with estimated mean fundamental frequency ($f_{H/V} \pm 1\sigma$) Hz and the mean H/V with 90% confidence intervals. ***a***, Site ALI; ***b***, Site HLG; ***c***, Site JLM; ***d***, Site KSP; ***e***, Site TMN; ***f***, Site NTI. Observed H/V are shown in light grey lines, mean H/V in red line, 90% CI in blue dotted lines and $\pm 1\sigma$ (standard deviation) in thick black lines.

for plateau such as peaks, may be treated as fundamental resonance frequency.

Some sites have shown clear peaks with low amplitude response, $H/V < 2$ such as MRG, NTI, GTH, most probably due to low contrast or compact structure. The sites that have shown flat responses such as BNK, PKH, KSL, SRP, LTA, as they are located on exposed bedrock. Along with stability, our consideration is for first

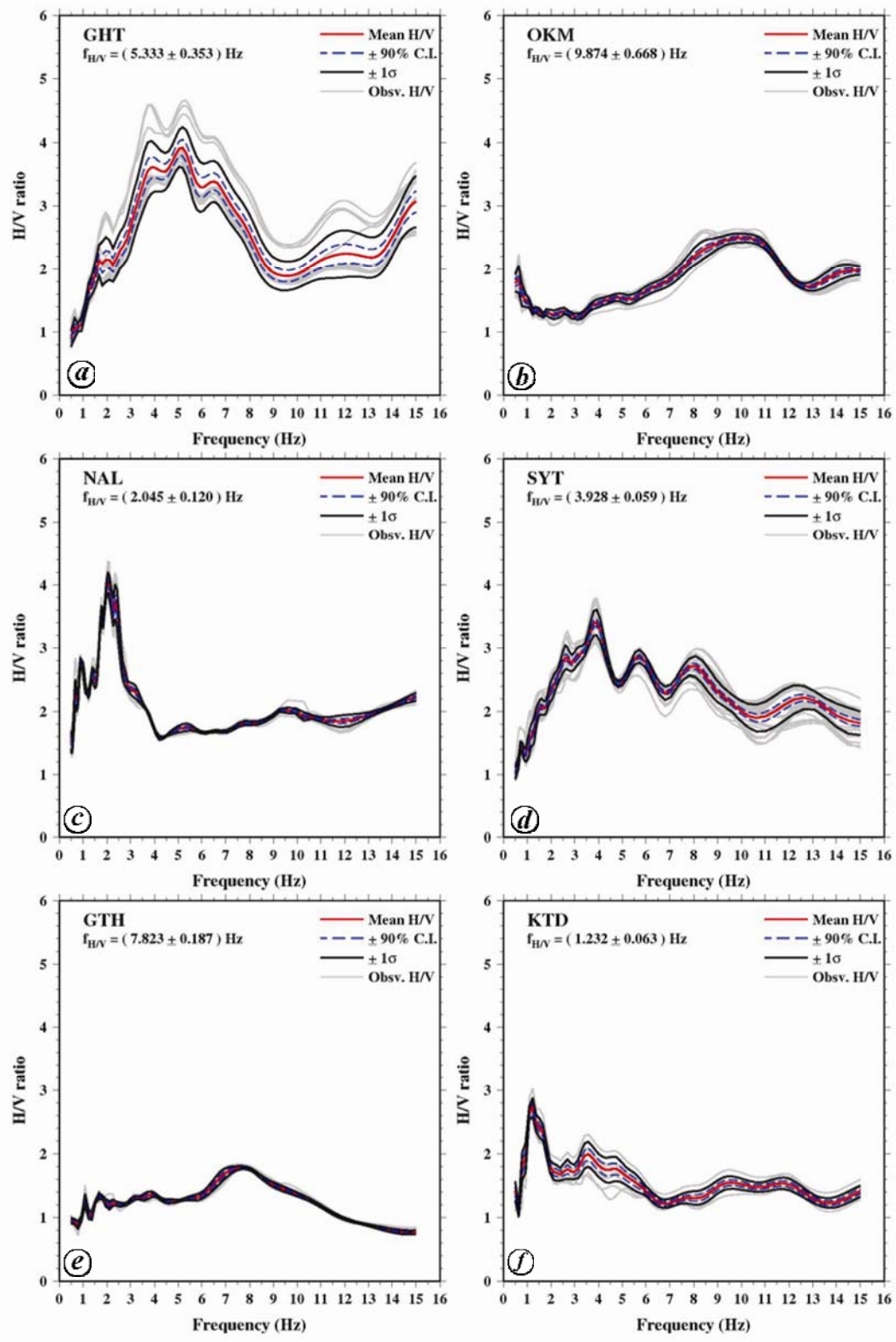

Figure 3. Sites located below MCT with estimated mean fundamental frequency ($f_{H/V} \pm 1\sigma$) Hz and the mean *H/V* with 90% confidence intervals. ***a***, Site GHT; ***b***, Site OKM; ***c***, Site NAL; ***d***, Site SYT; ***e***, Site GTH; ***f***, Site KTD.

approximations of site responses based on fundamental resonances, which presumably have close correspondence with 'natural soil frequency'. Examples of high site responses are sites such as GHT, JLM, TMN (as in Figures 3 *a*, 2 *c* and *e*), where, for site JLM, a high peak at 1.845 Hz, and trough at twice the frequency (i.e. at 3.69–4 Hz) are indicative of high Poisson's ratio[21]. High Poisson's ratio for top soil columns, indicative of high

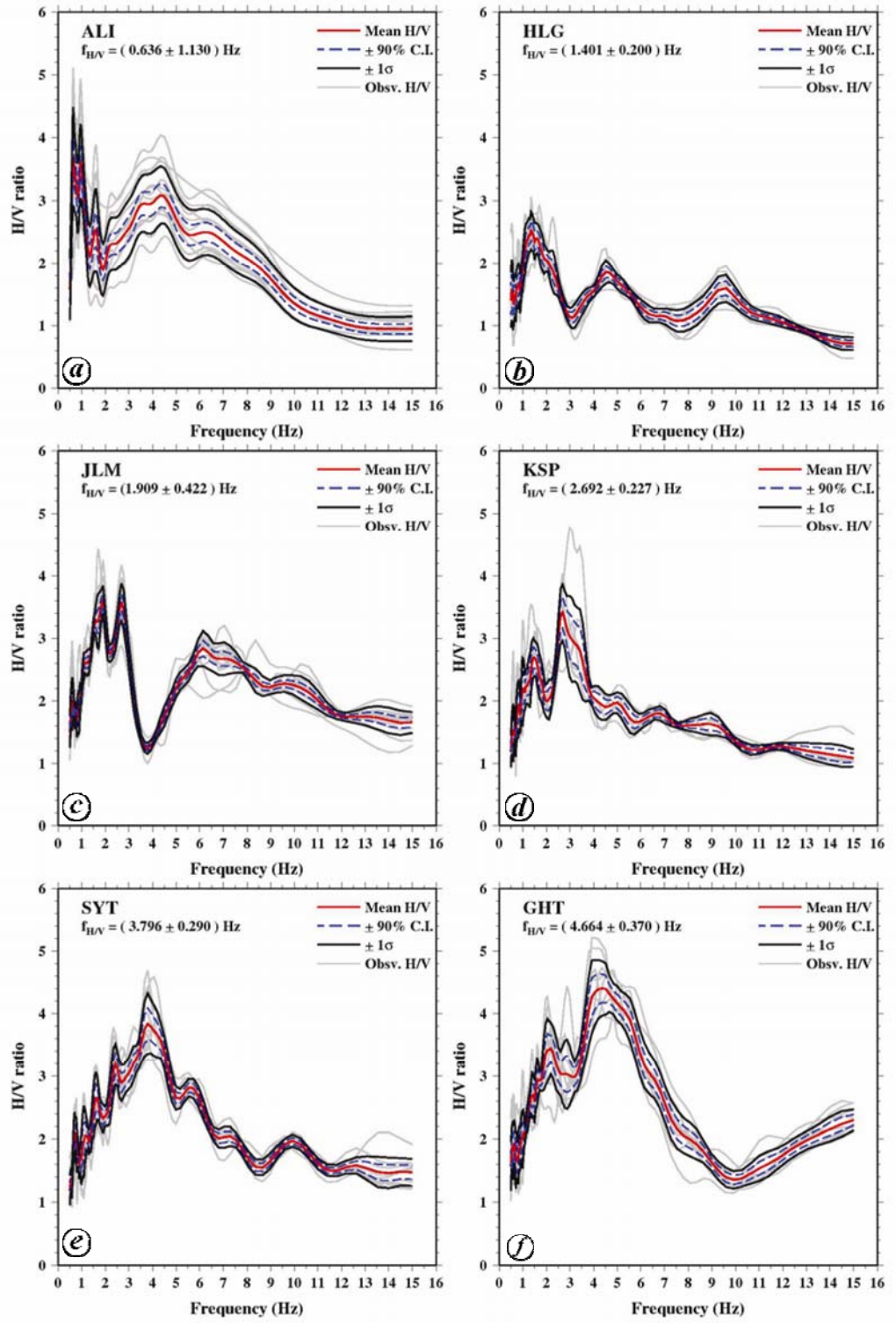

Figure 4. *H/V* ratios of earthquakes shown for a few sites. ***a***, ALI; ***b***, HLG; ***c***, JLM; ***d***, KSP; ***e***, SYT and ***f***, GHT.

unconsolidation (extremely clayey soil with high strain properties), may lead to severe ground motion and perhaps soil liquefaction. From another similar site response study by Nath *et al.*[9], around Chamoli region, GHT (GHAT) has indicated a high site amplification value 4.78 at 5 Hz. Our results indicate amplification level at 3.835 ± 0.145 (90% CI) at frequency 5.33 Hz.

A few experimental studies[22,23] have applied spectral ratio tests on earthquake data for site response estimation. In line with this method, we validated our ambient noise results by selecting a few local events recorded during the study period according to the USGS PDE list. Table 3 shows the list of selected 20 local earthquakes, having high signal-to-noise ratio recorded at the studied sites.

Table 3. Details of earthquakes taken from USGS PDE list, used for *H*/*V* ratio method, and recorded over our broadband seismograph network

Event no.	Origin time YYMMDD; hh mm ss	Latitude (°N)	Longitude (°E)	Depth (km)	Mb (USGS)
1	050905; 01 45 43.75	30.44	79.25	13.4	4.6
2	050916; 17 59 24.05	30.53	81.40	11.0	3.9
3	051025; 01 51 23.68	30.30	80.95	4.6	4.9
4	051214; 07 09 49.69	30.45	79.23	19.3	5.3
5	060201; 22 24 13.04	30.36	80.13	11.6	4.9
6	060214; 19 17 29.49	30.41	80.15	17.6	4.5
7	060421; 23 21 03.21	31.74	77.20	4.5	3.9
8	060507; 16 01 04.57	29.44	76.54	25.3	4.3
9	060718; 10 42 37.04	32.31	77.78	18.5	4.2
10	060720; 00 11 01.17	31.49	78.50	17.9	4.0
11	061112; 13 46 32.80	30.02	80.52	20.5	3.8
12	070129; 05 28 32.24	31.13	80.21	14.6	3.9
13	070203; 00 51 18.66	31.84	78.87	3.3	4.7
14	070221; 00 33 24.75	31.24	77.80	9.5	4.1
15	070310; 13 25 49.09	29.59	81.27	7.6	4.6
16	070327; 11 19 27.04	30.93	78.28	4.4	3.9
17	070614; 19 52 45.62	32.10	76.93	1.4	4.3
18	070620; 19 37 59.88	30.33	80.31	3.6	3.9
19	070722; 23 02 15.65	30.83	78.41	8.4	5.1
20	071125; 23 12 21.77	28.76	77.37	8.0	4.7

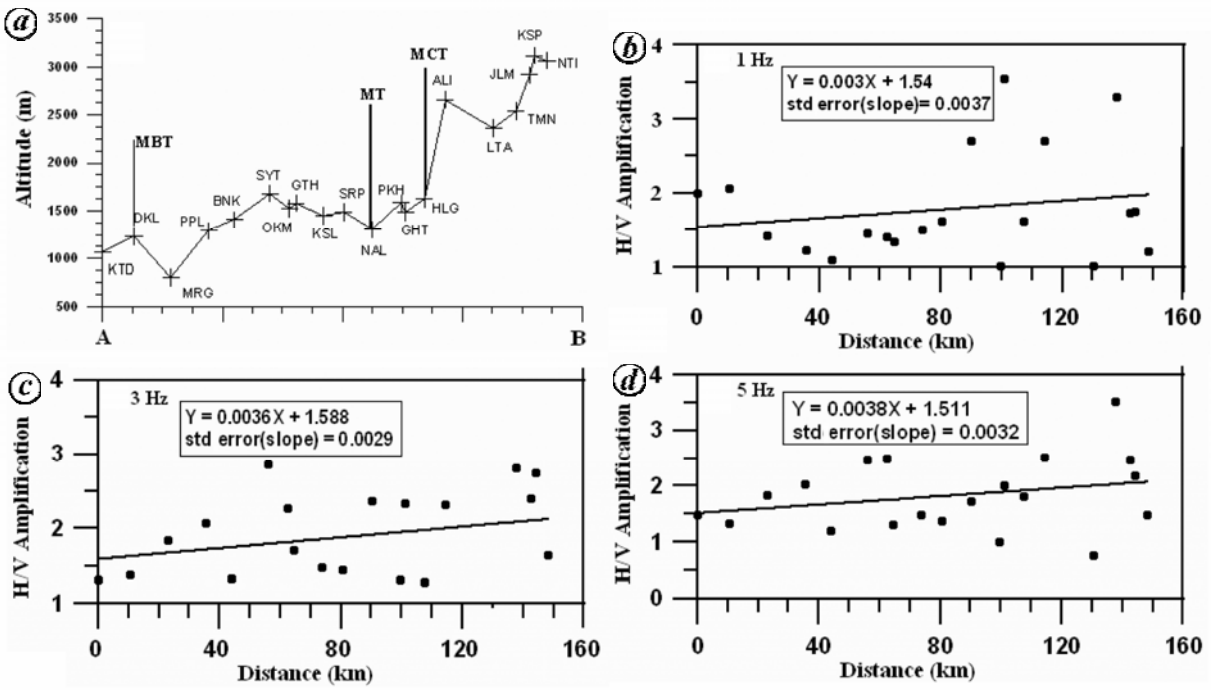

Figure 5. Trend of *H*/*V* amplification using ambient noise at different frequencies versus distance. ***a***, Cross-section of the study region; ***b***, at 1 Hz; ***c***, at 3 Hz; ***d***, at 5 Hz. The equation of the fitted straight line to the data points (circles) is shown in thick lines along with standard error of the slope (std error).

These were recorded at the stations during the study period and were selected for *H*/*V* ratios on the intense *S*-wave. Implementing instrumental response correction, FFT was calculated for a length of window including majority of the *S*-wave. The window length used for the calculation varied from 10 to 50 s. The window was tapered with a cosine taper of 0.05 bandwidth to avoid spectral leakage, the spectral amplitudes were logarithmically smoothed (Konno–Ohmachi) at moderate smoothing constant of 40 and *H*/*V* ratio was computed in the frequency range 0.5–15 Hz.

Observed and mean earthquake *H*/*V* ratios are shown for the sites in Figure 4. From the earthquake data, the resulting variability is shown with a mean *H*/*V* in red line, along with 90% CI (in blue dashed lines) and $\pm 1\sigma$ in thick black lines. In general, the earthquake *H*/*V* ratios

have shown slight frequency shifts in fundamental frequency estimates for sites with 'broad' peak curves, as compared to ambient noise, whereas clear peak sites have shown consistency in frequency estimates.

In the absence of detailed geotechnical information, the *H*/*V* method is able to detect the presence of soft-soil conditions, which provide conditions for site amplification from impedance changes and structural resonance. The small frequency shift between ambient noise and earthquake studies is probably due to the presence of other structural frequencies which are not damped-out in seismic motions.

All the study locations above and below the MT fault trace have shown an apparent site response in the 1–5 Hz frequency range, and more than 80% of the locations, not exceeding 5.5 Hz. We examined the cross-section of the study region from KTD to NTI for possible *H*/*V* amplification (*S*-wave) trend at different frequencies.

Figure 5 shows the possible amplification at 1, 3 and 5 Hz. The slope of the best fitting line and the standard error of the slope are also indicated. There are no discernible trends, as there is considerable scatter due to interstation distance; however, in the absence of concrete details pertaining to topographic amplification, these results may add some valuable information. Site directivity effects in the study region would be taken up in our further studies, to better characterize the topographical effect.

H/*V* ratios across the study region of Garhwal Himalaya have been applied to detect fundamental resonance frequencies for unknown rock profiles, using both ambient noise and earthquakes. Our study could predict unconsolidated sites, possible types of impedance contrasts, which may lead to site amplification from major earthquakes, due to low shear velocity and local structural resonance. Flat topography sites have shown clear *H*/*V* response, associated with well-defined fundamental site frequencies. Fundamental frequency estimates are observed mostly between 1 and 5 Hz. In general, we find that the empirical *H*/*V* method is a useful tool for preliminary site characterization and hazard analysis of the study locations, which seem to possess a high seismic risk in the eventuality of major earthquakes in the future.

1. Rajendran, K., Rajendran, C. P., Jain, S. K., Murty, C. V. R. and Arlekar, J. N., The Chamoli earthquake, Garhwal Himalaya: field observations and implications for seismic hazard. *Curr. Sci*., 2000, **78**, 45–51.
2. Gaur, V. K., Chander, R., Sarkar, I., Khattri, K. N. and Sinhval, H., Seismicity and state of stress from investigations of local earthquakes in the Kumaon Himalaya. *Tectonophysics*, 1985, **118**, 243–251.
3. Bilham, R., Gaur, V. K. and Molnar, P., Himalayan seismic hazard. *Science*, 2001, **293**, 1442–1444.
4. Khattri, K. N., Chander, R., Gaur, V. K., Sarkar, I. and Kumar, S., New seismological results on the tectonics of the Garhwal Himalaya. *Proc. Indian Acad. Sci. (Earth Planet. Sci.)*, 1989, **98**, 91–109.
5. Kayal, J. R., Singh, O. P., Chakraborty, P. K. and Karunakar, G., Aftershock sequence of the Chamoli earthquake of March 1999 in the Garhwal Himalaya. *Bull. Seismol. Soc. Am*., 2003, **93**, 109–117.
6. Rai, S. S., Ashish, Padhi, A. and Sharma, P. R., High crustal seismic attenuation in Ladakh–Karakoram. *Bull. Seismol. Soc. Am*., 2009, **99**, 407–415.
7. Nakamura, Y., A method for dynamic characteristics estimation of subsurface using microtremors on the ground surface. In Quarterly Reports of the Railway Technical Research Institute, Tokyo, 1989, vol. 30, pp. 25–33.
8. Lermo, J. and Chavez-Garcia, F. J., Are microtremors useful in site response evaluation? *Bull. Seismol. Soc. Am*., 1994, **84**, 1350–1364.
9. Nath, S. K., Sengupta, P. and Kayal, J. R., Determination of site response at Garhwal Himalaya from the aftershock sequence of 1999 Chamoli earthquake. *Bull. Seismol. Soc. Am.*, 2002, **92**, 1072–1081.
10. Gansser, A., *Geology of Himalayas*, Inter-Science Publisher, New York, 1964, p. 289.
11. Molnar, P. and Chen, W. P., Seismicity and mountain building. In *Mountain Building Processes* (ed. Hsü, K.), Academic Press, San Diego, CA, 1982, pp. 41–57.
12. Yin, A. and Harrison, T. M., Geologic evolution of the Himalayan–Tibetan orogen. *Annu. Rev. Earth Planet. Sci.*, 2000, **28**, 211–280.
13. Konno, K. and Ohmachi, T., Ground-motion characteristics estimated from spectral ratio between horizontal and vertical components of microtremor. *Bull. Seismol. Soc. Am*., 1998, **88**, 228–241.
14. Bard, P.-Y., Microtremor measurements: a tool for site effect estimation? In Proceedings of the Second International Symposium on the Effects of Surface Geology on Seismic Motion, Balkema, Rotterdam, Yokohama, Japan, 1–3 December 1998, vol. 3, pp. 1251–1279.
15. Bard, P.-Y. and SESAME-Team, Guidelines for the implementtation of the *H*/*V* spectral ratio technique on ambient vibrations – measurements, processing and interpretations, SESAME European research project EVG1-CT-2000–00026, deliverable D23.12, 2005; available at http://sesamefp5.obs.ujf-grenoble.fr
16. Bonnefoy-Claudet, S. *et al.*, Site effect evaluation in the basin of Santiago de Chile using ambient noise measurements. *Geophys. J. Int*., 2008, **176**, 925–937.
17. Dravinski, M., Ding, G. and Wen, K.-L., Analysis of spectral ratios for estimating ground motion in deep basins. *Bull. Seismol. Soc. Am*., 1996, **86**, 646–654.
18. Delgado, J., Casado, C.-L., Giner, J., Estevez, A., Cuenca, A. and Molina, S., Microtremor as a geophysical exploration tool: Application and limitations. *Pure Appl. Geophys*., 2000, **157**, 1445–1462.
19. Uebayashi, H., Extrapolation of irregular subsurface structures using the horizontal-to-vertical ratio of long-period microtremors. *Bull. Seismol. Soc. Am*., 2003, **93**, 570–582.
20. Guillier, B., Cornou, C., Kristek, J., Moczo, P., Bonnefoy-Claudet, S., Bard, P.-Y. and Fah, D., Simulation of seismic ambient vibrations: Does the *H*/*V* provide quantitative information in 2D-3D structures? In Proceedings of the Third International Symposium on the Effects of Surface Geology on Seismic Motion, Grenoble, France, 29 August–1 September 2006, p. 185.
21. Stephenson, W. R., Factors bounding prograde Rayleigh-wave particle motion in a soft-soil layer. In Proceedings of the 2003 Pacific Conference on Earthquake Engineering, New Zealand Society of Earthquake Engineering, Christchurch, New Zealand, 13–15 February 2003.
22. Lermo, J. and Chavez-Garcia, F. J., Are microtremors useful in site response evaluation? *Bull. Seismol. Soc. Am*., 1994, **84**, 1350–1364.
23. Parolai, S., Richwalski, S. M., Milkereit, C. and Bormann, P., Assessment of the stability of *H*/*V* spectral ratios from ambient noise and comparison with earthquake data in the Cologne area (Germany). *Tectonophysics*, 2004, **390**, 57–73.

Received 2 September 2012; revised accepted 11 July 2012